2003

Hypothalamic Proopiomelanocortin Neurons Are Glucose Responsive and Express KATP Channels

Nurhadi Ibrahim
Department of Physiology and Pharmacology

Martha A. Bosch
Department of Physiology and Pharmacology

James L. Smart
George Fox University, jsmart@georgefox.edu

Jian Qiu
Department of Physiology and Pharmacology

Marcelo Rubinstein
Instituto de Investigaciones en Ingenieria Genetica y Biologia Molecular

See next page for additional authors

Recommended Citation
Previously published in Endocrinology, 2003, 144(4), pp. 1331–1340 http://press.endocrine.org/doi/full/10.1210/en.2002-221033

Hypothalamic Proopiomelanocortin Neurons Are Glucose Responsive and Express K_{ATP} Channels

NURHADI IBRAHIM, MARTHA A. BOSCH, JAMES L. SMART, JIAN QIU, MARCELO RUBINSTEIN, OLINE K. RØNNEKLEIV, MALCOLM J. LOW, AND MARTIN J. KELLY

Department of Physiology and Pharmacology (N.I., M.A.B., J.Q., O.K.R., M.J.K.), The Vollum Institute (J.L.S., M.J.L.), and Department of Behavioral Neuroscience (M.J.L.), Oregon National Primate Research Center (O.K.R.), Oregon Health & Science University, Portland, Oregon 97239-3098; and Instituto de Investigaciones en Ingeniería Genética y Biología Molecular (M.R.), Consejo Nacional de Investigaciones Científicas y Técnicas, and Department of Biology, School of Sciences, University of Buenos Aires, Buenos Aires, Argentina

Hypothalamic proopiomelanocortin (POMC) neurons are critical for controlling homeostatic functions in the mammal. We used a transgenic mouse model in which the POMC neurons were labeled with enhanced green fluorescent protein to perform visualized, whole-cell patch recordings from prepubertal female hypothalamic slices. The mouse POMC-enhanced green fluorescent protein neurons expressed the same endogenous conductances (a transient outward K^+ current and a hyperpolarization-activated, cation current) that have been described for guinea pig POMC neurons. In addition, the selective μ-opioid receptor agonist DAMGO induced an outward current (maximum of 12.8 ± 1.2 pA), which reversed at K^+ equilibrium potential (E_{K+}), in the majority (85%) of POMC neurons with an EC_{50} of 102 nM. This response was blocked by the opioid receptor antagonist naloxone with an inhibition constant of 3.1 nM. In addition, the γ-aminobutyric $acid_B$ receptor agonist baclofen (40 μM) caused an outward current (21.6 ± 4.0 pA) that reversed at E_{K+} in these same neurons. The ATP-sensitive potassium channel opener diazoxide also induced an outward K^+ current (maximum of 18.7 ± 2.2 pA) in the majority (92%) of POMC neurons with an EC_{50} of 61 μM. The response to diazoxide was blocked by the sulfonylurea tolbutamide, indicating that the POMC neurons express both Kir6.2 and sulfonylurea receptor 1 channel subunits, which was verified using single cell RT-PCR. This pharmacological and molecular profile suggested that POMC neurons might be sensitive to metabolic inhibition, and indeed, we found that their firing rate varied with changes in glucose concentrations. Therefore, it appears that POMC neurons may function as an integrator of metabolic cues and synaptic input for controlling homeostasis in the mammal.

THE MEDIOBASAL HYPOTHALAMUS (MBH) contains the largest concentration of proopiomelanocortin (POMC) neurons in the central nervous system (1–3). These POMC neurons project to regions throughout the forebrain (3). Two of the major posttranslational products of MBH POMC neurons, β-endorphin (β-END) and α-MSH, have been associated with many physiological functions including reproduction, metabolic homeostasis, stress responses, and natural reward (4–6). At the cellular level, the opioid peptide β-END has been shown to postsynaptically modulate the excitability of local γ-aminobutyric acid (GABA) and dopamine neurons (7–9). In addition, GnRH, oxytocin, and vasopressin neurosecretory (8) neurons are inhibited by β-END (10–13). The other putative neurotransmitter of POMC neurons, αMSH, has been shown to modulate synaptic input to paraventricular neurons that are thought to be involved in the regulation of metabolic homeostasis (14).

The opioid peptide β-END modulates target neurons through a G protein-coupled receptor. The μ-opioid receptor is $G\alpha_{i/o}$-coupled to either the activation of an inwardly-rectifying K^+ channel (Kir3.1–3.4, GIRKs), the inhibition of adenylyl cyclase, or the inhibition of Ca^{2+} channels (15). The GIRK-type subfamily of inwardly rectifying K^+ channels comprises four different channel subtypes, all of which are expressed in the rat hypothalamus (16). Hypothalamic neurons are inhibited through a μ-opioid receptor that is coupled to GIRKs (7, 12, 17–19).

ATP-sensitive potassium (K_{ATP}) channels are another member of the inwardly-rectifying K^+ channel family (20). They are heteromultimeric complexes of sulfonylurea receptors (SUR; the regulatory subunit) and inwardly rectifying K^+ channel (Kir6.1–6.2) subunits (21, 22). These channel complexes couple membrane excitability to cellular metabolism by directly sensing and integrating intracellular changes in the concentration of nucleotides (23). The Kir6.2 plus SUR1 channel complex is activated by diazoxide and by metabolic inhibition and is blocked with high affinity by sulfonylureas such as glibenclamide and tolbutamide (23). Sulfonylurea binding and electrophysiological studies have characterized neuronal K_{ATP} channels in a variety of neurons. For example, Kir6.2 is widely distributed in rat brain and is present in neurons expressing tyrosine hydroxylase, neuropeptide Y, and glutamic acid decarboxylase (24).

In the rat hypothalamus, the adipocyte hormone leptin hyperpolarizes glucose-responsive, ventromedial nucleus

Abbreviations: aCSF, Artificial cerebrospinal fluid; DAMGO, D-Ala^2, *N*-Me-Phe^4, Gly-ol^5-enkephalin; DEPC, diethylpyrocarbonate; EGFP, enhanced green fluorescent protein; E_{K+}, equilibrium potential; β-END, β-endorphin; GABA, γ-aminobutyric acid; GIRK, G protein-coupled inwardly rectifying K^+ channel; HBSS, Hanks' balanced salt solution; I_A, a transient outward K^+ current; I_h, hyperpolarization-activated, cation current; I/V, current/voltage; K_{ATP}, ATP-sensitive potassium; Kir, inwardly rectifying K^+ channels; MBH, mediobasal hypothalamus; POMC, proopiomelanocortin; RT, reverse transcriptase; SUR, sulfonylurea receptors; TTX, tetrodotoxin.

neurons via activation of a K^+ current that is blocked by tolbutamide (25). Also, insulin hyperpolarizes glucose-responsive neurons via a tolbutamide-sensitive K^+ current (26). More recent studies have shown that these glucose-responsive neurons express Kir6.2 and SUR1 transcripts (27), which renders them diazoxide and tolbutamide sensitive. Previous findings suggest that the G protein-coupled receptors such as the dopamine D_2, $GABA_B$, and somatostatin SST_5 receptors are coupled to both GIRKs and Kir6.2 in pancreatic β-cells and substantia nigra neurons (28, 29). However, the relationship between expression of GIRKs and Kir6.2 channel subtypes in hypothalamic neurons is not known. Because POMC neurons are so critical for regulating homeostasis and motivated behaviors in the mammal (6, 30), we hypothesized that POMC neurons would respond to activators of GIRKs and Kir6.2 channels and serve as integrators of both synaptic and hormonal (metabolic) input. We used a transgenic mouse model in which we could visualize enhanced green fluorescent protein (EGFP)-labeled POMC neurons and measure the direct effects of the μ-opioid agonist DAMGO, the K_{ATP} channel opener diazoxide and metabolic inhibition.

Materials and Methods

POMC-EGFP transgenic mice

Transgenic mice were generated on an inbred C57BL/6 genetic background as previously described (31). All animals for these studies were maintained under controlled temperature (25 C) and photoperiod conditions (14-h light, 10-h dark; lights on between 0530 and 1930) with food and water *ad libitum*. The animal procedure protocols were done in accordance with the NIH Guide for the Care and Use of Laboratory Animals and were approved by our local animal care and use committee. Based on the immunocytochemical staining of fixed tissue sections through the arcuate nucleus, greater than 99% of the EGFP-tagged neurons contained β-END, and there were over 3000 POMC neurons counted in each hypothalamus (31). Therefore, we were confident that we could target POMC neurons based on the presence of EGFP expression in a hypothalamic slice preparation.

Electrophysiology

Female POMC-EGFP transgenic mice (14–21 d) were selectively bred in-house, and maintained under the conditions described above. On the day of experiment, the mice were anesthetized with halothane, decapitated, the brain rapidly removed from the skull and a block containing the hypothalamus immediately dissected. (The trunk blood was collected, and serum estrogen levels determined by chromatography and subsequent RIA by Oregon National Primate Research Center. Serum estrogen levels in these immature female mice were 5.9 ± 0.8 pg/ml, which were significantly below castrate levels of adult females.) The hypothalamic block was submerged in cold (4 C) oxygenated (95% O_2, 5% CO_2) artificial cerebrospinal fluid (aCSF) with low Ca^{2+} containing the following constituents, in mM: NaCl, 124; KCl, 5; $NaHCO_3$, 26; NaH_2PO_4, 2.6; dextrose, 10; HEPES, 10; $MgSO_4$, 2; $CaCl_2$, 1. Coronal slices (300 μm) through the caudal-rostral extent of the arcuate nucleus were cut with a vibratome during which time (20 min) the slices were bathed in aCSF with low Ca^{2+} at 4 C. The arcuate slices were then transferred to an auxiliary chamber where they were kept at room temperature (25 C) in aCSF with normal Ca^{2+} (2 mM) until recording (recovery ~1.5 h), at which time a single slice was transferred to the recording chamber. Once in the recording chamber, the slices were kept viable by continually perfusing with warm (35 C), oxygenated normal aCSF at 1.5 ml/min.

For imaging and recording, slices were viewed with a Zeiss Axioskop outfitted for fluorescence (fluorescein isothiocyanate filter) and infrared differential interference contrast videomicroscopy. After visualizing fluorescent POMC-EGFP neurons with the 5× objective, a 40× water immersion objective was used for infrared differential interference contrast imaging to visualize neurons for whole-cell patch clamp recording. Microelectrodes (resistances 3–6 MΩ) were fabricated from borosilicate glass pipettes (1.5 mm OD) and filled with an internal solution (pH 7.30) containing the following constituents, in mM: K-gluconate, 128; NaCl, 10; $MgCl_2$, 2; EGTA, 11; HEPES, 10; ATP, 1; GTP, 0.25. Standard whole-cell voltage clamp procedures were followed using an Axopatch 200A amplifier (2-kHz lowpass filter, Axon Instruments, Union City, CA) as previously described (32). Signals were digitized with a Digidata 1200, and analyzed using pClamp 7.0 software (Axon Instruments). The liquid junctional potential of −10 mV was corrected in the data analysis. Current and voltage traces were also recorded on a analog chart recorder (Gould Instruments, Valley View, OH).

Following formation of a greater than 1 GΩ seal, intracellular access was achieved by suction, followed by perfusion with 1 μM tetrodotoxin (TTX, Alomone Labs, Jerusalem, Israel) for at least 4–6 min to block spontaneous firing and action potential-generated synaptic potentials. All the responses to agonists and antagonists were measured in voltage clamp (V_{hold} = −60 mV) with the exception of the glucose experiments. The access resistance was checked before and after each drug treatment, and only those cells that showed less than 10% change in access resistance throughout the recording were included in this study. The access varied from 20–30 MΩ ($\bar{x}$ = 24.4 ± 0.8 MΩ), which ensured adequate voltage clamp of this slow outward K^+ current and minimal rundown during pharmacological testing due to rapid dialysis of intracellular (second messenger) constituents.

For the cell attached recordings, the patch pipettes were filled with the external solution (aCSF), and a loose seal (100 MΩ) was formed on the identified POMC neurons to measure spontaneous activity in current clamp. After a stable baseline was established after several minutes of recording, the glucose concentration was rapidly decreased from 10–5 mM. The firing activity was measured over a minute period after stabilization and compared with the firing rate measured 1 min before the change in the glucose concentration. Only cells that showed a full recovery were used to calculate the change in firing frequency with altered glucose concentrations.

Drug application

Following generation of a control current-voltage plot in the presence of TTX, drugs were perfused until a steady-state outward current was obtained. Diazoxide (7-chloro-3-methyl-2H-1,2,4-benzo-thiadiazin 1,1-dioxide) and tolbutamide (Sigma, St. Louis, MO) were dissolved in dimethylsulfoxide 99.5% to a stock concentration of 300 mM and 100 mM, respectively. Perfusion of aCSF containing 0.1–0.3% dimethylsulfoxide (vehicle controls) had no effect on the cells. Naloxone (Sigma) and DAMGO (D-Ala^2, *N*-Me-Phe^4, Gly-ol^5-enkephalin; Peninsula Laboratories, Inc., Belmont, CA) were dissolved in Milli-Q H_2O to a stock concentration of 1 mM. Baclofen (Sigma) was dissolved in 0.1 N HCl to a concentration of 40 mM. Aliquots of the stock solutions were stored appropriately until needed. Final drug concentrations were made up in 10 ml volumes and perfused at 1.5 ml/min. On the average, it took 2–5 min to reach a steady-state outward current with DAMGO, baclofen, or diazoxide. The drug-induced change in conductance was determined by subtracting the pre- from the postdrug current/voltage (I/V) slopes. Composite dose-response curves were generated from the following logistic equation fitted by computer (Origin 4.1, Microcal) to the data: $\Delta I_{max} = 100 \cdot ([agonist]^n/([agonist]^n + EC_{50}{}^n))$, where ΔI_{max} is the maximum outward current for a given agonist, EC_{50} represents the agonist potency, and n is the Hill slope.

The pharmacodynamics sometimes were reevaluated after the drug wash-out in the presence of antagonists. Estimates of the K_i for antagonists were derived from the logistic equation fitted by computer (SigmaPlot 2000, Jandel Scientific) to the data: $\Delta I_{max} = 100 \cdot ([agonist]^n/([agonist]^n + (EC_{50}{}^n \cdot (1 + ([antagonist]^n/K_i{}^n)))))$.

Acutely dispersed neurons

For these experiments, we prepared hypothalamic slices from adult Topeka guinea pigs using the same procedures as for the preparation of mouse hypothalamic slices (see above). The 300-μm coronal hypothalamic slices were cut on a vibratome from caudal to rostral and placed in an auxiliary chamber containing oxygenated, normal aCSF. The slices were allowed to recover for 1–2 h in the chamber before dispersion. The

arcuate nucleus of the hypothalamus was microdissected and incubated in 2–3 ml of Hanks' balanced salt solution [HBSS (in mM): $CaCl_2$,1.26; $MgSO_4$,1; KCl, 5.37; KH_2PO_4, 0.44; NaCl,136.89; Na_2HPO_4, 0.34; D-glucose, 5.55; HEPES,15 in diethylpyrocarbonate (DEPC)-treated water, pH 7.3, 300 mOsm] containing 1 mg/ml protease XIV (Sigma) for approximately 15 min at 37 C. The tissue was then washed four times in one volume low calcium aCSF and two times in HBSS. The cells were isolated by trituration with flame-polished pasteur pipettes, dispersed on a 35-mm Petri dish and continuously perfused with HBSS at a rate of 1.5 ml/min. Cells were visualized using an inverted microscope, and individual neurons were patched and harvested into the patch pipette by applying negative pressure. The content of the pipette was expelled into a siliconized microcentrifuge tube containing 5 μl of the following solution: 0.5 μl of 10× buffer (100 mM Tris-HCl, 500 mM KCl, 1% Triton X-100; Promega Corp., Madison, WI), 15 U RNasin (Promega Corp.), 0.5 μl 100 mM dithiothreitol, and DEPC-treated water.

Tissue total RNA purification

Hypothalamic tissue was homogenized and total RNA extracted using the RNeasy kit (QIAGEN, Valencia, CA) according to the manufacturer's protocol. Total RNA was treated with deoxyribonuclease I, which was then inactivated and removed using DNA-free reagents as described by the manufacturer (Ambion, Inc., Austin, TX). The RNA was diluted and used as a positive (+ reverse transcriptase [+RT]) or negative (−RT) control for the PCRs.

RT-PCR of single cells and tissue RNA

The harvested cell solution and 25 ng of hypothalamic total RNA in 1 μl were denatured for 5 min at 65 C then cooled on ice for 5 min. Single-stranded cDNA was synthesized from cellular RNA by adding 50 U murine leukemia virus RT (Applied Biosystems, Foster City, CA), 1.5 μl 10× buffer, 2 mM $MgCl_2$, 0.2 μM deoxynucleotide triphosphate, 15 U RNasin, 10 mM dithiothreitol, 100 ng random hexamers, and DEPC-treated water to a final volume of 20 μl. Cells and tissue RNA used as negative controls, were processed as described above but without RT. The reaction mixtures were incubated at 42 C for 60 min, denatured at 99 C for 5 min, and cooled on ice for 5 min.

PCR was performed using 2–3 μl of cDNA template from each RT reaction in a 30-μl PCR volume containing: 3 μl 10× buffer, 2.4 μl $MgCl_2$ (2 mM final concentration for POMC, Kir6.1, and SUR1) or 4.8 μl $MgCl_2$ (4 mM final concentration for Kir6.2), 0.2 mM deoxynucleotide triphosphate, 0.2 μM forward and reverse primers, 2 U Taq DNA polymerase (Promega Corp.), and 0.22 μg TaqStart Antibody (CLONTECH Laboratories, Inc., Palo Alto, CA). Taq DNA polymerase and TaqStart Antibody were combined and incubated at room temperature for 5 min, the remainder of the reaction contents were added to the tube and incubated at 94 C for 2 min. Then, each reaction went through 60 cycles of amplification according to the following protocols: 94 C, 45 sec (denaturation); 60 C, 45 sec (annealing); 72 C, 1 min 10 sec (elongation), with a final 72 C extension for 5 min (POMC, Kir6.1, and SUR1) or 94 C, 45 sec (denaturation); 68 C, 1 min (annealing and elongation combined), with a final 72 C extension for 5 min (Kir6.2). Ten microliters of the PCR products were visualized with ethidium bromide on a 1.5% agarose gel.

The primers used were as follows: guinea pig POMC; 344-bp product (accession no. S78260), forward primer (bases 40–60) 5′-CTGGCCTTGCTGCTTCAGAT-3′; reverse primer (bases 383–363) 5′-ATGGAGTAGGAGCGCTTGTC-3′. Guinea pig Kir6.2; 398-bp product (accession no. AF183920), forward primer (bases 1608–1627) 5′-GCCCGCTTTGTGTCCAAGAA-3′; reverse primer (bases 2005–1985) 5′-CCCAGCATGATGGCGTTGAT-3′. Guinea pig SUR1; 238-bp product (accession no. AF183921), forward primer (bases 1325–1345) 5′-GCCACGGCTTCCATCGACAT-3′; reverse primer (bases 1562–1542) 5′-CGCTGGCAGGTCACTTGTCT-3′. Guinea pig Kir6.1; 220-bp product (accession no. AF183918), forward primer (bases 379–399) 5′-GGACATCTACGCTTACATGG-3′; reverse primer (bases 598–578) 5′-GACAGCGTTGATGATCAGAC-3′. Guinea pig glyceraldehyde-3 phosphate dehydrogenase (GAPDH); 212-bp product (accession no. CPU51572), forward primer (bases 123–143)5′CATCCACTGGTGCTGCCAAG-3′; reverse primer (bases 334–314) 5′-GTCCTCGGTGTAGCCCAAGA-3′. Primers were synthesized by Invitrogen (Carlsbad, CA), and the optimum PCR conditions for each primer pair was established in preliminary experiments. The PCR product from single cells for each primer pair was sequenced in our core facilities.

Results

Passive membrane properties and endogenous conductances

Initially, whole cell recordings were made from 103 POMC-EGFP neurons from prepubertal female mice (C57BL/6J background) using visualized, whole-cell patch recording. We were confident that all of the cells that we targeted were POMC neurons based on a previous study in which 99% of the neurons expressing EGFP were identified as β-END neurons (31). For the electrophysiology analysis, only POMC cells with gigaohm or better seals were included in this study. The mean resting membrane potential was -55.4 ± 2.2 mV at a 0 pA holding current, and the mean input resistance was 1.1 ± 0.1 GΩ. Moreover, the majority (68%) of female mouse POMC neurons exhibited the same endogenous conductances that we have described in female guinea pig POMC neurons under low steroid (ovariectomized) conditions, which included expression of a hyperpolarization-activated, cation current (I_h) and a transient outward K^+ current (I_A; Fig. 1). Hence, the passive membrane properties of mouse POMC neurons labeled with EGFP are similar to what we have reported for guinea pig and rat POMC neurons identified *post hoc* by immunocytochemistry (17, 18). Therefore, we do not think that the EGFP expression in POMC neurons altered the physiological properties of these neurons.

Coupling of μ-opioid receptor to GIRK: effects of DAMGO

Based on our previous findings in guinea pig POMC neurons that indicated the μ-opioid receptor mediates autoinhibition of these opioid neurons, we evaluated the coupling of the μ-opioid receptor to GIRK in mouse POMC-EGFP neurons. In the presence of TTX (1 μM), DAMGO (30–1000 nM) induced an outward current in 54 out of 63 (85%) of mouse POMC neurons. DAMGO (1 μM) caused a maximum outward current of 12.8 ± 1.2 pA (n = 22) that reversed near E_{K+} ($E_{DAMGO} = -81.0 \pm 2.5$ mV *vs.* $E_{K+} = -84.5$ mV) and increased the whole-cell slope conductance by 1.3 ± 0.2 nS (Fig. 2). Moreover, the nonselective opioid receptor antagonist naloxone attenuated the response to DAMGO (Fig. 2). A concentration-response relationship was generated from 54 neurons, and the majority of POMC neurons were tested with a single concentration of DAMGO. In addition, a small number of POMC neurons were tested with two concentrations of DAMGO, a lower concentration followed by a higher concentration of agonist to establish a maximum (outward current) response within a given cell. A logistics equation fit to the data points yielded an EC_{50} of 102.8 nM (Fig. 3).

In an additional 22 POMC neurons, the DAMGO-induced outward current was antagonized by the opioid receptor antagonist naloxone. A single concentration of DAMGO (300–3000 nM) was applied to each neuron in the presence of 20 nM naloxone. The antagonism by naloxone produced a rightward shift in the agonist dose-response curve with an estimated K_i of 3.1 nM (Fig. 3). This K_i for naloxone inhibition of μ-opioid response is similar to what we and others have published for naloxone antagonism of μ-opioid receptor-mediated responses in the central nervous system (33, 34).

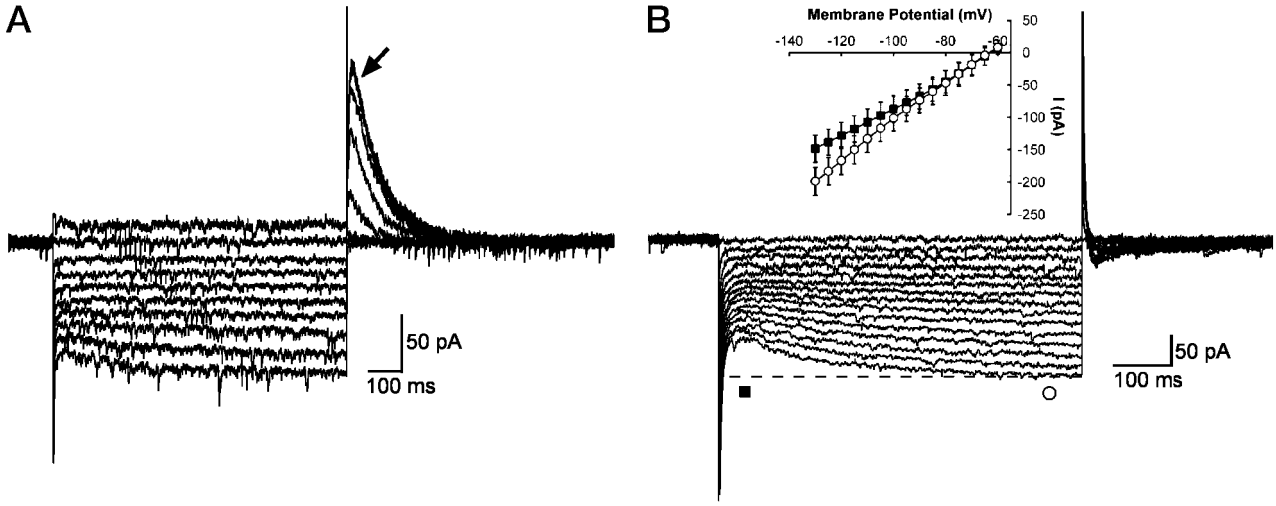

FIG. 1. Female mouse POMC-EGFP neurons express I_A and I_h currents. A, Transient outward currents (I_A, *arrow*) generated in a whole-cell recording of a mouse EGFP-POMC neuron elicited by holding the cell at −60 mV and giving a series of 1-sec prepulses ranging from −50 mV to −140 mV (in 10 mV increments) and stepping back to −60 mV. Resting V_m = −54 mV. B, I_h generated in mouse POMC-EGFP neuron. This current has the appearance of a sag (*dotted line*) following the instantaneous current observed at the onset of the hyperpolarizing voltage command. The cell was held at −60 mV and given a series of hyperpolarizing pulses from −65 to −130 mV (5-mV increments for 600 msec). Resting V_m = −60 mV. The *inset graph* is the composite I/V curve (leak subtracted) showing the differences between the instantaneous and steady-state inward current for POMC neurons with the symbols on the current traces showing where the instantaneous (■) and the steady-state (○) currents were measured.

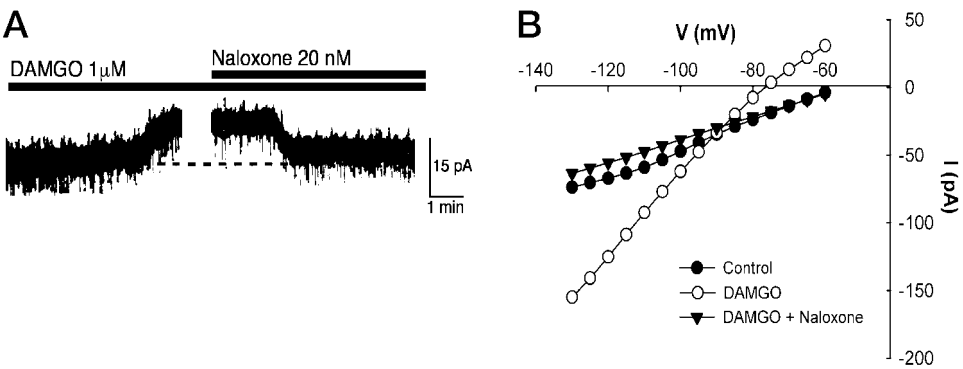

FIG. 2. Female mouse POMC neurons respond to μ-opioid receptor agonist DAMGO. A, In the presence of 1 μM TTX, bath application of DAMGO induced a 15-pA outward current. This effect was blocked by opioid receptor antagonist naloxone (20 nM). The break in the recording trace indicates where I/V data were obtained. V_{hold} = −60 mV (resting V_m = −62 mV). The *dotted line* in this figure and subsequent figures serves as a point of reference only. B, The pre-DAMGO, post-DAMGO, and post-DAMGO + naloxone current-voltage relationships from another POMC neuron. The reversal potential for the outward current was close to the predicted equilibrium potential for potassium (E_{DAMGO} = −90 mV).

$GABA_B$ receptor agonist baclofen activates GIRK

We have shown that guinea pig POMC neurons are inhibited by both DAMGO and the $GABA_B$ receptor agonist baclofen via activation of GIRKs (35). Therefore, we tested mouse POMC neurons to see if they would show a similar response to the $GABA_B$ receptor agonist baclofen. Indeed, all of the mouse POMC cells that were sensitive to DAMGO responded to the $GABA_B$ receptor agonist baclofen (40 μM) with an outward current (21.6 ± 4.0 pA) that reversed near E_{K+} ($E_{baclofen}$ = −80.7 ± 7.2 mV, n = 8) and with an increase in slope conductance of 1.8 ± 0.5 nS (Fig. 4). Therefore, it appears that the $GABA_B$ receptor is similarly coupled to activation of GIRK as the μ-opioid receptor in mouse POMC neurons. Further elucidation of the $GABA_B$-mediated response was not undertaken because we have extensively characterized this response in guinea pig and rat hypothalamic neurons (18, 35–38).

Activation of Kir6.2 by the K_{ATP} channel opener diazoxide

Based on the RT-PCR detection of both Kir6.2 and SUR1 transcripts in the mediobasal hypothalamus of the mouse (27), we hypothesized that mouse POMC neurons express Kir6.2 and SUR1 and therefore would be sensitive to the K_{ATP} channel opener diazoxide and the sulfonylurea drug tolbutamide. Following perfusion with TTX (1 μM), diazoxide (3–1000 μM) induced an outward current in 37 out of 40 (92%) mouse POMC neurons. Diazoxide (300 μM) caused a maximum outward current of 18.7 ± 2.2 pA (n = 9) that reversed at E_{K+} ($E_{Diazoxide}$ = −82.5 ± 1.8 mV) and increased the slope conductance by 1.5 ± 0.1 nS (Fig. 5). Moreover, the SUR1 selective drug tolbutamide antagonized the actions of diazoxide at equimolar concentrations (n = 12, Fig. 4). A concentration-response relationship for diazoxide was generated, using a single concentration of diazoxide to test each POMC neuron. A logistics equation fit to the data

yielded an EC_{50} of 61.3 μM (Fig. 6). We did not see any evidence for desensitization of the diazoxide response even at concentrations of the drug that gave a maximum response (300–1000 μM).

Activation of Kir6.2 and GIRK in mouse POMC neurons

Based on the response of POMC neurons to DAMGO and diazoxide, we asked whether the same cells could respond to both agonists and therefore exhibit an additive response (*i.e.* a greater maximum outward current). Therefore, we recorded from an additional 27 POMC neurons from prepubertal female mice. Based on the response to both agonists, there were three distinct subpopulations of POMC neurons. In over 50% of the cells (n = 14), there was an additive effect of both drugs such that the maximum outward current generated by diazoxide added to a maximum outward current produced by DAMGO (Fig. 7A). In fact, 9 of 14 cells showed an additive response that was not significantly different from the theoretical maximum based on both channels (GIRK and Kir6.2) being activated (27.7 ± 2.8 pA *vs.* 31.5 ± 2.2 pA). The additive response did not depend on the order of drug application. The other five cells of this subpopulation showed an additive response to perfusion of DAMGO followed by diazoxide (n = 3) or diazoxide followed by DAMGO (n = 2) that was less than the theoretical maximum additive response (13.8 ± 0.7 pA *vs.* 31.5 ± 1.2 pA). POMC neurons that responded to both drugs were not localized to any particular region (rostral *vs.* caudal) of the mediobasal hypothalamus.

In another subpopulation of POMC neurons, DAMGO induced a large outward current (24.4 ± 2.0 pA, n = 8) without any further effect of diazoxide (Fig. 7B). A third subpopulation showed a robust diazoxide-induced outward current (18.2 ± 1.1 pA, n = 5) without any further effect of DAMGO (Fig. 7C). Again, the order of drug perfusion did not make any difference in terms of the responses, and the responses did not appear to be region specific. In addition, we did not see a specific effect of tolbutamide to block the DAMGO-activated GIRK (n = 5) or the opioid receptor antagonist naloxone to block the diazoxide response (n = 2) in POMC neurons. Therefore, there appeared to be three distinct subpopulations of mouse POMC neurons. One population responded to both μ-opioid receptor activation by DAMGO, coupling to GIRK, and K_{ATP} channel activation by diazoxide. Another population responded to μ-opioid activation only; and finally, a smaller population of POMC neurons responded to the K_{ATP} channel opener diazoxide only.

Although there is evidence for activation of GIRK and K_{ATP} channels by G protein-coupled receptors (28, 29), we did not see any evidence of a direct activation of K_{ATP} channels by DAMGO. However, over a longer time period there could be a change in activity of K_{ATP} channels due to $G\alpha_{i/o}$ inhibition of adenylyl cyclase activity.

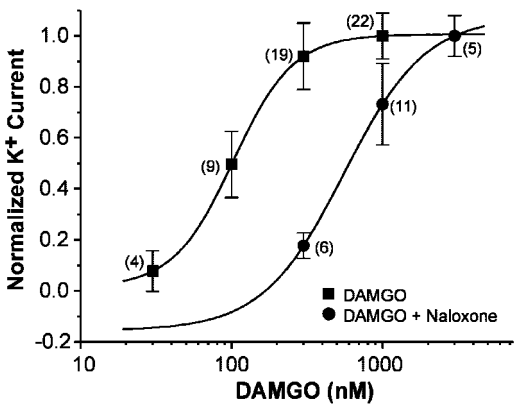

FIG. 3. Concentration-response curves for DAMGO and antagonism by naloxone. DAMGO (30–1000 nM) induced outward K^+ currents in female POMC neurons in a dose-dependent manner. *Squares* represent the means, and the *bars* SEMs for each concentration of DAMGO normalized to the maximum outward current (12.8 ± 2.2 pA, n = 54). The number of neurons tested at each concentration is given in *parentheses*. Based on a logistics equation fit to the data points (see *Materials and Methods*), the EC_{50} for DAMGO was 102.8 nM. Naloxone (20 nM) antagonized the response to DAMGO and shifted the EC_{50} to 555.8 nM with an estimated K_i of 3.1 nM (n = 22). The *circles* represent the means, and the *bars* SEMs for each concentration of DAMGO in the presence of naloxone normalized to the maximum response.

Expression of Kir6.2 and SUR1 transcripts in POMC neurons

The electrophysiological data on the potency of diazoxide to induce an outward K^+ current in POMC cells suggested that POMC cells express Kir6.2 subunits. Also, the sensitivity

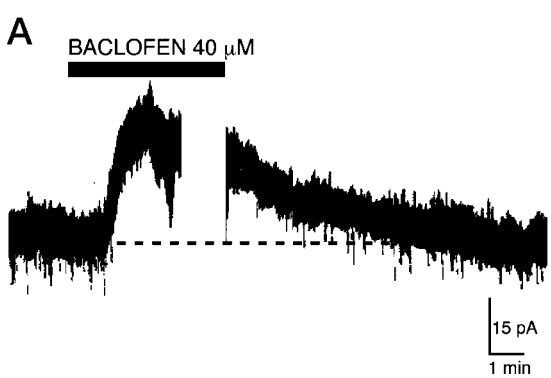

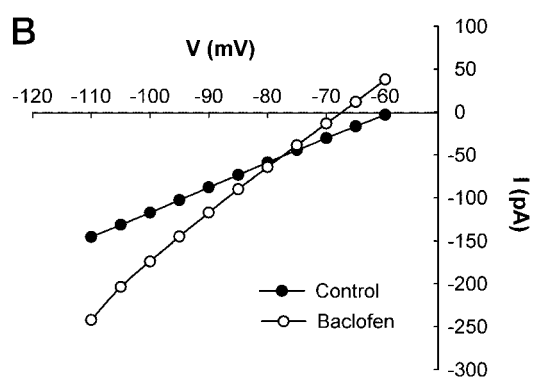

FIG. 4. Female mouse POMC neurons respond to the $GABA_B$ agonist baclofen. A, In the presence of TTX (1 μM), perfusion of baclofen (40 μM) induced a 20-pA outward current. This cell also responded to DAMGO (see Fig. 2). The break in the recording indicates where current-voltage data were obtained. V_{hold} = −60 mV (resting V_m = −54 mV). B, I/V relationships for another POMC neuron that responded to baclofen. The baclofen-induced outward current that reversed near E_{K+} ($E_{baclofen}$ = −78 mV).

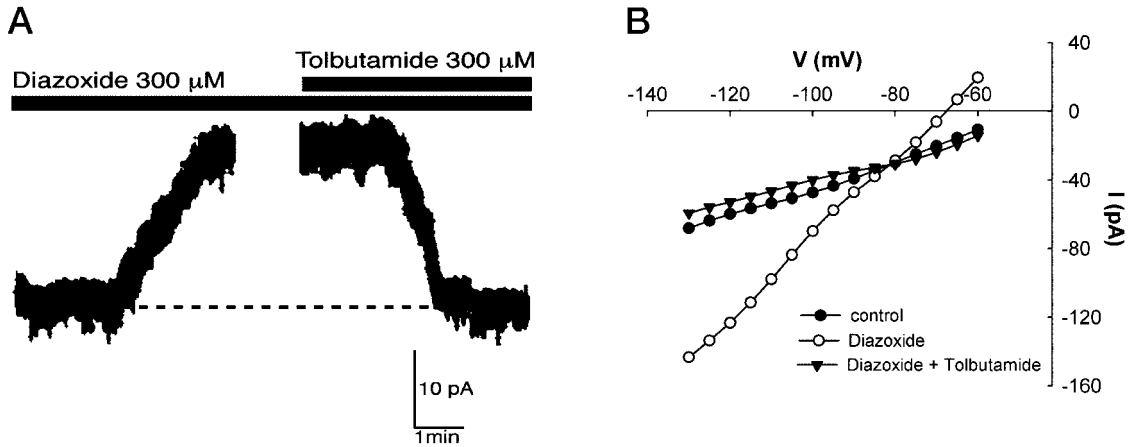

FIG. 5. Female mouse POMC neurons respond to the K_{ATP} channel opener diazoxide. A, In the presence of TTX, a POMC neuron responded to the K_{ATP} channel opener diazoxide (300 μM) with 20 pA outward current. This effect was reversed by the sulfonylurea tolbutamide (300 μM). The break in the recording trace indicates where I/V data were obtained. V_{hold} = −60 mV (resting V_m = −50 mV). B, The predizoxide, postdiazoxide, and postdiazoxide + tolbutamide current-voltage relationships from the POMC neuron in panel A. The reversal potential for the outward current was close to the predicted equilibrium potential for potassium ($E_{diazoxide}$ = −85 mV).

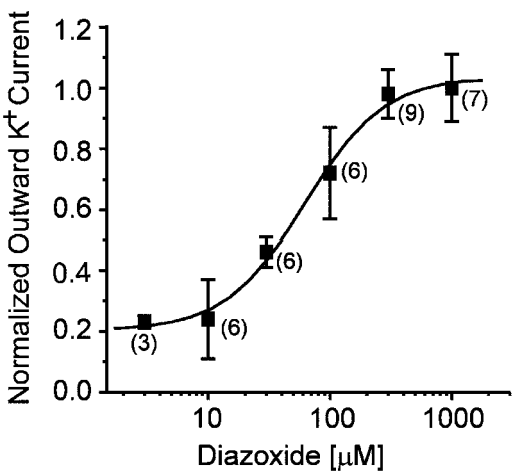

FIG. 6. Concentration-response curve for the K_{ATP} channel opener diazoxide. Diazoxide (30–1000 μM) induced outward K^+ currents in female POMC neurons in a dose-dependent manner. *Squares* represent the means, and the *bars* SEMs for each concentration of diazoxide normalized to the maximum outward current (18.7 ± 2.2 pA, n = 37). The number of cells for each concentration is given in parenthesis. Based on a logistics equation fit to the data points (see *Materials and Methods*), the EC_{50} for diazoxide was 61.3 μM.

of this response to tolbutamide antagonism suggested that SUR1 is the sulfonylurea receptor subunit within the K_{ATP} channel. To define the molecular composition of the K_{ATP} channel directly, we measured the expression of transcripts using single cell RT-PCR. These experiments were carried out in dispersed guinea pig POMC neurons in which we have measured an equivalent pharmacological response to diazoxide and tolbutamide and have specific primers for Kir6.1, Kir6.2, SUR1, and POMC. The PCR product from single cells for each primer was sequenced and found to be specific. In addition, the specificity of the single cell PCR products had been verified in preliminary experiments using real-time PCR (39). Based on previous electrophysiological recordings from the caudal mediobasal hypothalamus (17, 36, 40), we predicted that POMC neurons make up about 20% of the population. Indeed, in our analysis of 20 arcuate neurons that were dispersed, patched and then harvested for RT-PCR, four POMC neurons were identified, three of which expressed Kir6.2 and SUR1 (Fig. 8). Although adjacent neurons also expressed Kir6.1, Kir6.2 and SUR1 transcripts, Kir6.2 plus SUR1 appear to be the predominant transcripts expressed in arcuate neurons (Fig. 8), which agrees with our pharmacological profile for the K_{ATP} channel in these neurons.

POMC neurons are glucose responsive

The fact that POMC neurons express Kir6.2 and SUR1 transcripts and are sensitive to diazoxide and tolbutamide suggested that they would be directly modulated by metabolic signals. However, the expression of Kir6.2 plus SUR1 transcripts is necessary but not sufficient for sensing changes in glucose (41). Therefore, we measured the direct response to changes in glucose concentrations. For these experiments, we did cell attached recordings from mouse POMC neurons to monitor the firing rate and reduced the extracellular concentrations of glucose within physiological limits (42). Reduction in extracellular concentrations of glucose from 10 mM to 5 mM significantly decreased the baseline firing rate to 41.5 ± 7.7% in 10 of 12 POMC cells, whereas it did not affect the firing rate (91.8 ± 8.2%, n = 4) of adjacent, unidentified arcuate neurons (Fig. 9). The spontaneous firing rate returned to control levels in all of the POMC neurons; however, the time course of recovery from metabolic inhibition varied among POMC neurons. Therefore, although the changes in the firing rate of POMC neurons may be due in part to altered synaptic input, the direct expression of K_{ATP} channels and the sensitivity to glucose suggests that POMC neurons are glucose-responsive neurons (*i.e.* they increase their firing rate in response to increases in glucose concentrations).

Discussion

To our knowledge, this is the first study showing that POMC neurons express a complement of inwardly rectifying

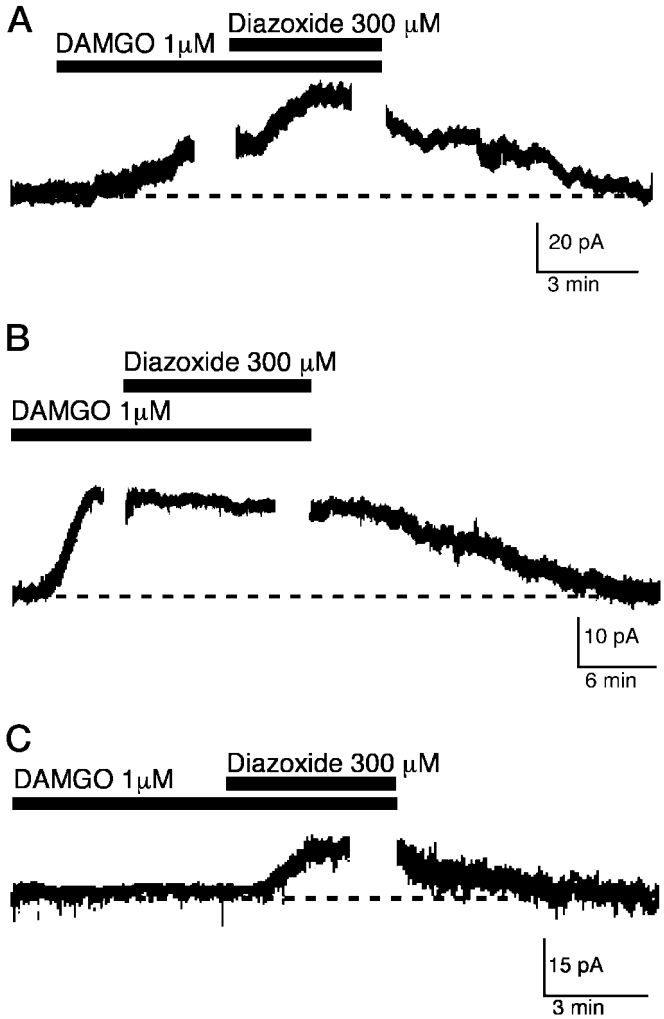

FIG. 7. Three populations of POMC neurons based on their response to DAMGO and diazoxide. A, The effects of DAMGO and diazoxide were additive in the majority of female mouse POMC neurons. Diazoxide (300 μM) produced an additional 22-pA outward current when coperfused with DAMGO (1 μM), which generated a maximal outward current of 18 pA in the presence of 1 μM TTX. The breaks in the recording trace indicates points where current/voltage data were obtained. $V_{hold} = -60$ mV (resting $V_m = -54$ mV). B, A subpopulation of female POMC neurons responded to DAMGO only. Coperfusion of diazoxide (300 μM) did not augment to maximal outward current produced by 1 μM DAMGO (25 pA) in the presence of 1 μM TTX. The breaks in the recording trace indicates points where current/voltage data were obtained. $V_{hold} = -60$ mV (resting $V_m = -51$ mV). C, A subpopulation of female POMC neurons responded to diazoxide only. Diazoxide (300 μM) induced maximal outward current of 15 pA in the presence of 1 μM TTX following the application of 1 μM DAMGO, which had no effect in this POMC neuron. The break in the recording trace indicates when current/voltage data were obtained. $V_{hold} = -60$ mV (resting $V_m = -57$ mV).

potassium channels that allows them to be sensitive to both neurotransmitter (opioids and GABA) input and metabolic cues. Furthermore, we have found that POMC neurons express Kir6.2 and SUR1 transcripts and are glucose responsive. In addition, we have identified two other distinct populations of POMC neurons that were responsive either to μ-opioid receptor activation or to K_{ATP} channel openers only. The fact that there are three subpopulations of POMC neurons is not surprising in view of the fact that these command neurons of the hypothalamus are involved in almost every aspect of hypothalamic control of homeostasis. Indeed, POMC neurons have been associated with many physiological functions including control of the ovulatory cycle and reproductive behavior, metabolic homeostasis, fluid balance, stress responses, and motivated behaviors. One of the mediators of many of these functions is β-END, which is a posttranslational product of POMC.

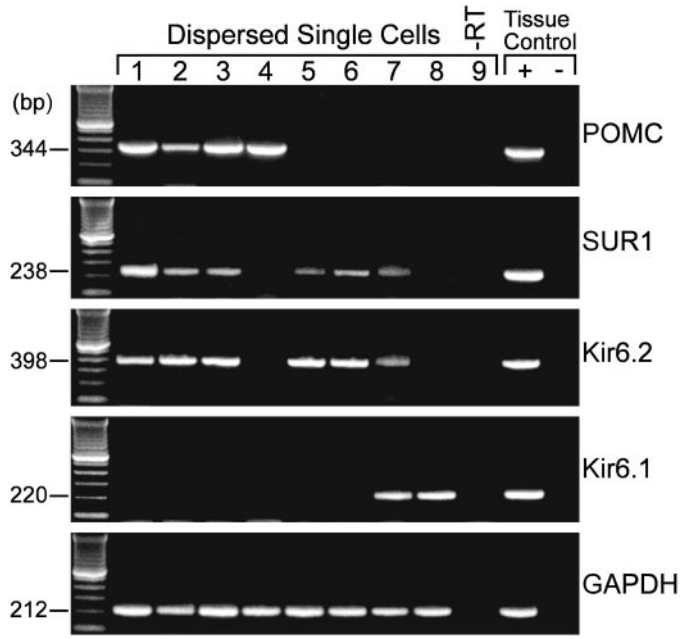

FIG. 8. Kir6.2 and SUR1 transcripts are detected in POMC neurons. RT-PCR analysis of Kir6.2, Kir6.1, and SUR1 transcripts in single cells harvested from dispersed arcuate neurons from the guinea pig. The expected size of the PCR products is indicated, and the single-cell PCR products were verified with sequencing. GAPDH transcripts were analyzed in the same cells as an internal control for the RT reaction. The following controls were also included: HBSS from the recording chamber; a water blank (B) and basal hypothalamic (BH) tissue RNA all of which were reversed transcribed in the presence of RT (+RT). In addition, a single cell and tissue RNA were included that were processed without RT (−RT). PCR was performed for 60 cycles.

Acting through $G\alpha_{i/o}$-coupled μ-opioid receptors, β-END can inhibit its target neurons through activation of GIRK, inhibition of adenylyl cyclase or inhibition of Ca^{2+} channels (15). At the cellular level, μ-opioid receptor agonists have been shown to modulate the excitability of dopamine neurons (7), GnRH neurons (10, 12), oxytocin and vasopressin neurons (13) and finally local GABA neurons (37). In addition, we have demonstrated that mediobasal hypothalamic POMC neurons are similarly self-inhibited through a μ-opioid autoreceptor that is coupled to GIRK activation (17). In fact, the μ-opioid receptor agonist DAMGO is more potent (EC_{50} 60 nM) but equally efficacious in hyperpolarizing female guinea pig POMC neurons (40) as mouse POMC neurons. However, the present findings indicate that DAMGO is more potent to hyperpolarize POMC neurons (102 nM) *vs.* other arcuate neurons (315 nM) in the C57BL/6J strain of mice (19).

The $GABA_B$ receptor is also coupled to GIRK channels in

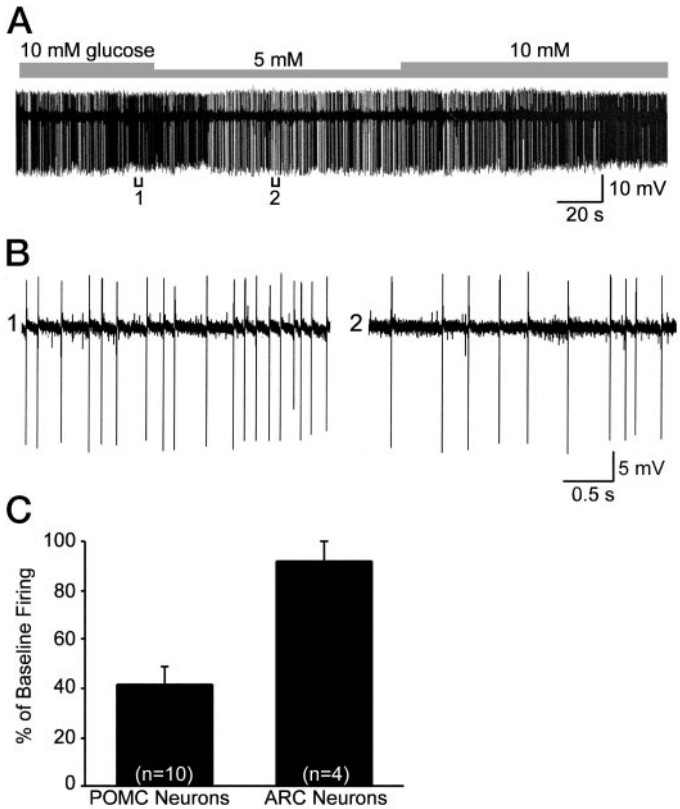

FIG. 9. POMC neurons are glucose responsive. A, Reduction in extracellular concentrations of glucose from 10 mM to 5 mM significantly decreased the firing rate of a POMC neuron recorded in the cell-attached mode. The cell fully recovered to its original baseline firing rate. B, Expansion of chart record in *A* shows that the spontaneous firing rate decreased from 6 Hz (bracket 1) to about 3 Hz (bracket 2) or a 50% reduction in firing. C, Summary of the decrease in the spontaneous firing rate in POMC *vs.* unidentified, adjacent arcuate neurons following a reduction in the glucose concentration from 10 to 5 mM. *Bars* represent the mean, and *lines* 1 SEM of the baseline firing rate. Eighty percent (10 of 12) of the POMC neurons were inhibited by a reduction in glucose concentration.

guinea pig POMC neurons (35), and we have found a similar coupling in mouse POMC neurons. This indicates that GABA input from local arcuate GABA/NPY neurons would also provide a powerful inhibitory tone onto these POMC neurons via $GABA_B$ receptors (18, 31, 36), which is thought to play an important role in inhibiting POMC neurons during activation of feeding circuits (43).

On the other hand, K_{ATP} channels couple membrane excitability to cellular metabolism by directly sensing and integrating intracellular concentration changes of nucleotides such as ATP and ADP (20). Sulfonylurea binding and electrophysiological studies have characterized neuronal K_{ATP} channels with different properties in a variety of cell types, including hippocampal and midbrain neurons. Kir6.2 is widely distributed in rat brain, and is present in neurons expressing tyrosine hydroxylase, NPY and glutamic acid decarboxylase (24, 27, 39). Presently, our electrophysiological findings together with the single cell RT-PCR indicate that POMC neurons also express Kir6.2. In fact, the EC_{50} for diazoxide is similar to what has been reported for pancreatic β-cells (44) and rat hippocampal pyramidal neurons (51 μM; Ref. 45). Based on the sensitivity to tolbutamide and single cell RT-PCR data, hypothalamic POMC neurons also appear to express SUR1. Liss and colleagues (46, 47) have shown that GABAergic neurons in the substantia nigra pars recticularis show a similar K_{ATP} channel subunit profile, with Kir6.2 and SUR1 coexpression detected in the majority of the neurons. In all cases, Kir6.2 plus SUR1-K_{ATP} channels are activated by diazoxide and by metabolic inhibition, and are blocked with high affinity by sulfonylureas such as tolbutamide. In addition, we have found that another SUR1-selective antagonist, glipizide, potently blocks the diazoxide response in POMC neurons (unpublished observations).

One of the classical feeding centers of the hypothalamus is the ventromedial nucleus in which resides glucose-responsive neurons, *i.e.* neurons that increase their firing in response to elevations in blood glucose levels (48–50). Based on recent single cell RT-PCR experiments, ventromedial glucose-responsive neurons express Kir6.2 plus SUR1 subunits (27). Therefore, it appears that glucose-responsive neurons can transduce, via the K_{ATP} channel, changes in extracellular glucose levels to changes in neuronal excitability. Based on our single cell RT-PCR results, arcuate guinea pig POMC neurons also express this same compliment of K_{ATP} channel subunits. In preliminary experiments with specific primers to mouse Kir6.2, we have found that the majority of dispersed mouse POMC-EGFP neurons express Kir6.2. However, the expression of Kir6.2 plus SUR1 is necessary but not sufficient for sensing changes in glucose (41). Therefore, it is important that we have found that a small reduction in extracelluar concentrations of glucose significantly inhibited POMC cell firing, whereas adjacent non-POMC neurons were not affected even though some of these may express Kir6.2 and SUR1 mRNA. It is also known that POMC neurons express glucokinase, which is a necessary enzyme for glucose-sensing cells (51). So, in addition to activation by leptin (31, 52), POMC neurons appear to be glucose responsive.

It is not surprising that we have identified three subpopulations of POMC neurons based on their reponse to μ-opioid agonists and K_{ATP} channel openers. In addition to their role in energy homeostasis (43, 53, 54), POMC neurons have multiple other functions including regulating reproduction (12, 55), parturition (13), fluid balance (56), stress responses (4, 6), and natural reward (5, 30, 57). Because of their involvement in all these different functions, POMC neurons are thought to be the "command" neurons of the hypothalamus. Perhaps part of the diversity in the POMC neurons lies in the differential processing of POMC to α-MSH, which is prominent in feeding circuits, and to β-END, which is involved in modulating reproduction, stress and natural rewards. In addition, POMC neurons are located in the arcuate and periarcuate region including the median eminence, which is outside the blood brain barrier. Therefore, they are in a strategic location for sensing humoral signals and translating these signals into neural activity.

For example, we have found that POMC neurons respond rapidly to estrogen, which serves to inhibit GnRH neurons during the negative feedback phase of the ovulatory cycle (12, 58). Perhaps another subset of POMC neurons respond rapidly to changing levels of leptin and/or glucose to translate these metabolic cues into neural signals. Interestingly,

earlier studies in the female rat demonstrated that glucose-responsive neurons in the ventromedial nucleus were also sensitive to the acute actions of estrogen, which depolarized these cells via a cAMP-dependent pathway (59). Because we know that estrogen is anorexic (60) and activates POMC neurons in the female guinea pig via protein kinase A (34), the steroid may synergize with leptin and glucose to inhibit feeding in the female. Electrophysiology experiments are currently underway to measure the response of mouse POMC neurons to estrogen since there are profound gender differences in the control of metabolic homeostasis (60).

In summary, we have found that POMC neurons express a unique complement of inwardly rectifying K^+ channels (GIRKs, Kir6.2) and SUR proteins that allow them to respond to metabolic (*e.g.* glucose) changes and synaptic input (*e.g.* GABA/NPY neurons). In addition, we know that the synaptic input to POMC neurons can be modulated by gonadal steroids and that leptin can directly excite these cells through activation of a cation-selective current. Therefore, these POMC neurons are uniquely situated to respond to ascending sensory input, metabolic changes and hormonal fluctuations that enable them to integrate multiple inputs and serve as the command neurons of the hypothalamus to maintain homeostasis in the mammal.

Acknowledgments

Received October 7, 2002. Accepted December 20, 2002.

Address all correspondence and requests for reprints to: Martin J. Kelly, Ph.D., Department of Physiology and Pharmacology, L334, Oregon Health Sciences University, 3181 Southwest Sam Jackson Park Road, Portland, Oregon 97239-3098. E-mail: kellym@ohsu.edu.

This work was supported by Public Health Service Grants DA-05158, DA-00192 (Research Scientist Development Award, to M.J.K.), NS-38809, NS-35944, DK-55819, HG-00201, and the International Scholar Program of the Howard Hughes Medical Institute.

References

1. **Elde RP, Hökfelt T** 1979 Localization of hypophysiotropic peptides and other biologically active peptides within the brain. Annu Rev Physiol 41:587–602
2. **Khachaturian H, Lewis ME, Haber SN, Akil H, Watson SJ** 1984 Proopiomelanocortin peptide immunocytochemistry in rhesus monkey brain. Brain Res Bull 13:785–800
3. **Khachaturian H, Lewis ME, Shafer MKH, Watson SJ** 1985 Anatomy of the CNS opioid systems. Trends Neurosci 8:111–119
4. **Millan MJ, Herz A** 1985 The endocrinology of the opioids. Int Rev Neurobiol 26:1–83
5. **Di Chiara G, North RA** 1992 Neurobiology of opiate abuse. Trends Pharmacol Sci 131:185–193
6. **Rubinstein M, Mogil JS, Japón M, Chan EC, Allen RG, Low MJ** 1996 Absence of opioid stress-induced analgesia in mice lacking β-endorphin by site-directed mutagenesis. Proc Natl Acad Sci USA 93:3995–4000
7. **Loose MD, Rønnekleiv OK, Kelly MJ** 1990 Membrane properties and response to opioids of identified dopamine neurons in the guinea pig hypothalamus. J Neurosci 10:3627–3634
8. **Horvath TL, Naftolin F, Leranth C** 1992 β-Endorphin innervation of dopamine neurons in the rat hypothalamus: a light and electron microscopic double immunostaining study. Endocrinology 131:1547–1555
9. **Gribble FM, Loussouarn G, Tucker SJ, Zhao C, Nichols CG, Ashcroft FM** 2000 A novel method for measurement of submembrane ATP concentration. J Biol Chem 275:30046–30049
10. **Thind KK, Goldsmith PC** 1988 Infundibular gonadotropin-releasing hormone neurons are inhibited by direct opioid and autoregulatory synapses in juvenile monkeys. Neuroendocrinology 47:203–216
11. **Goldsmith PC, Boggan JE, Thind KK** 1991 Opioid synapses on vasopressin neurons in the paraventricular and supraoptic nuclei of juvenile monkeys. Neuroscience 45:709–719
12. **Lagrange AH, Rønnekleiv OK, Kelly MJ** 1995 Estradiol-17β and μ-opioid peptides rapidly hyperpolarize GnRH neurons: a cellular mechanism of negative feedback? Endocrinology 136:2341–2344
13. **Russell JA, Leng G, Bicknell RJ** 1995 Opioid tolerance and dependence in the magnocellular oxytocin system: a physiological mechanism. Exp Physiol 80:307–340
14. **Cowley MA, Pronchuk N, Fan W, Inulescu DM, Colmers WF, Cone RD** 1999 Integration of NPY, AGRP, and melanocortin signals in the paraventricular nucleus of the hypothalamus: evidence of a cellular basis for the adipostat. Neuron 24:155–163
15. **North RA** 1993 Opioid actions on membrane ion channels. In: Herz A, ed. Handbook of experimental pharmacolgy: opioid I. New York: Springer-Verlag; 773–797
16. **Karschin C, Dissmann E, Stuhmer W, Karschin A** 1996 IRK(1–3) and GIRK(1–4) inwardly rectifying K+ channel mRNAs are differentially expressed in the adult rat brain. J Neurosci 16:3559–3570
17. **Kelly MJ, Loose MD, Rønnekleiv OK** 1990 Opioids hyperpolarize β-endorphin neurons via μ-receptor activation of a potassium conductance. Neuroendocrinology 52:268–275
18. **Loose MD, Rønnekleiv OK, Kelly MJ** 1991 Neurons in the rat arcuate nucleus are hyperpolarized by $GABA_B$ and μ-opioid receptor agonists: evidence for convergence at a ligand-gated potassium conductance. Neuroendocrinology 54:537–544
19. **Slugg RM, Hayward MD, Rønnekleiv OK, Low MJ, Kelly MJ** 2000 Effect of the μ-opioid agonist DAMGO on medial basal hypothalamic neurons in β-endorphin knockout mice. Neuroendocrinology 72:208–217
20. **Reimann F, Ashcroft FM** 1999 Inwardly rectifying potassium channels. Curr Opin Cell Biol 11:503–508
21. **Clement IV JP, Kunjilwar K, Gonzalez G, Schwanstecher M, Paten U, Aguilar-Bryan L, Bryan J** 1997 Association and stoichiometry of K_{ATP} channel subunits. Neuron 18:827–838
22. **Ashcroft FM, Gribble FM** 1998 Correlating structure and function in ATP-sensitive K+ channels. Trends Neurosci 21:288–294
23. **Ashcroft FM, Gribble FM** 2000 New windows on the mechanism of action of K_{ATP} channel openers. Trends Pharmacol Sci 21:439–445
24. **Dunn-Meynell AA, Rawson NE, Levin BE** 1998 Distribution and phenotype of neurons containing the ATP-sensitive K^+ channel in rat brain. Brain Res 814:41–54
25. **Spanswick D, Smith MA, Groppi VE, Logan SD, Ashford MLJ** 1997 Leptin inhibits hypothalamic neurons by activation of ATP-sensitive potassium channels. Nature 390:521–525
26. **Spanswick D, Smith MA, Mirshamsi S, Routh VH, Ashford ML** 2000 Insulin activates ATP-sensitive K^+ channels in hypothalamic neurons of lean, but not obese rats. Nat Neurosci 3:757–758
27. **Miki T, Liss B, Minami K, Shiuchi T, Saraya A, Kashima Y, Horiuchi M, Ashcroft F, Minokoshi Y, Roeper J, Seino S** 2001 ATP-sensitive K^+ channels in the hypothalamus are essential for the maintenance of glucose homeostasis. Nat Neurosci 4:507–512
28. **Roeper J, Hainsworth AH, Ashcroft FM** 1990 Tolbutamide reverses membrane hyperpolarisation induced by activation of D2 receptors and $GABA_B$ receptors in isolated substantia nigra neurones. Pflugers Arch 416:473–475
29. **Smith PA, Sellers LA, Humphrey PP** 2001 Somatostatin activates two types of inwardly rectifying K+ channels in MIN-6 cells. J Physiol 532:127–142
30. **Hayward MD, Pintar JE, Low MJ** 2002 Selective reward deficit in mice lacking β-endorphin and enkephalin. J Neurosci 22:8251–8258
31. **Cowley MA, Smart JL, Rubinstein M, Cerdán MG, Diano S, Horvath TL, Cone RD, Low MJ** 2001 Leptin activates anorexigenic POMC neurons through a neural network in arcuate nucleus. Nature 411:480–484
32. **Wagner EJ, Rønnekleiv OK, Kelly MJ** 2001 The noradrenergic inhibition of an apamin-sensitive, small conductance Ca^{2+}-activated K^+ channel in hypothalamic γ-aminobutyric acid neurons: pharmacology, estrogen sensitivity and relevance to the control of the reproductive axis. J Pharmacol Exp Ther 299:21–30
33. **Williams JT, North RA** 1984 Opiate-receptor interactions on single locus coeruleus neurones. Mol Pharmacol 26:489–497
34. **Lagrange AH, Rønnekleiv OK, Kelly MJ** 1997 Modulation of G protein-coupled receptors by an estrogen receptor that activates protein kinase A. Mol Pharmacol 51:605–612
35. **Lagrange AH, Wagner EJ, Rønnekleiv OK, Kelly MJ** 1996 Estrogen rapidly attenuates a $GABA_B$ response in hypothalamic neurons. Neuroendocrinology 64:114–123
36. **Kelly MJ, Loose MD, Rønnekleiv OK** 1992 Estrogen suppresses μ-opioid and $GABA_B$-mediated hyperpolarization of hypothalamic arcuate neurons. J Neurosci 12:2745–2750
37. **Wagner EJ, Bosch MA, Kelly MJ, Rønnekleiv OK** 1999 A powerful $GABA_B$ receptor-mediated inhibition of GABAergic neurons in the arcuate nucleus. Neuroreport 10:2681–2687
38. **Wagner EJ, Rønnekleiv OK, Bosch MA, Kelly MJ** 2001 Estrogen biphasically modifies hypothalamic GABAergic function concomitantly with negative and positive control of luteinizing hormone release. J Neurosci 21:2085–2093
39. **Bosch MA, Qiu J, Ibrahim N, Kelly MJ, Rønnekleiv OK** 2001 Whole-cell patch-clamp recording and single-cell RT-PCR analysis of K-ATP channel expression in guinea pig hypothalamic arcuate neurons. Soc Neurosci Abstr 733.9
40. **Lagrange AH, Rønnekleiv OK, Kelly MJ** 1994 The potency of μ-opioid hy-

perpolarization of hypothalamic arcuate neurons is rapidly attenuated by 17β-estradiol. J Neurosci 14:6196–6204
41. **Levin BE** 2002 Metabolic sensors. Viewing glucosensing neurons from a broader perspective. Physiol Behav 76:397–401
42. **Silver IA, Erecinska M** 1994 Extracellular glucose concentration in mammalian brain: continuous monitoring of changes during increased neuronal activity and upon limitation in oxygen supply in normo-, hypo-, and hyperglycemic animals. J Neurosci 14:5068–5076
43. **Williams G, Bing C, Cai XJ, Harrold JA, King PJ, Liu XH** 2001 The hypothalamus and the control of energy homeostasis: different circuits, different purposes. Physiol Behav 74:683–701
44. **Babenko AP, Aguilar-Bryan L, Bryan J** 1998 A view of SUR/K_{IR}6. X, K_{ATP} channels. Annu Rev Physiol 60:667–687
45. **Matsumoto N, Komiyama S, Akaike N** 2002 Pre- and postsynaptic ATP-sensitive potassium channels during metabolic inhibition of rat hippocampal CA1 neurons. J Physiol 541:511–520
46. **Liss B, Bruns R, Roeper J** 1999 Alternative sulfonylurea receptor expression defines metabolic sensitivity of K-ATP channels in dopaminergic midbrain neurons. EMBO J 18:833–846
47. **Liss B, Roeper J** 2001 A role for neuronal K_{ATP} channels in metabolic control of the seizure gate. Trends Pharmacol Sci 22:599–601
48. **Oomura Y, Ono T, Ooyama H, Wayner MJ** 1969 Glucose and osmosensitive neurones of the rat hypothalamus. Nature 222:282–284
49. **Minami T, Oomura Y, Sugimori M** 1986 Electrophysiological properties and glucose responsiveness of guinea-pig ventromedial hypothalamic neurones in vitro. J Physiol (London) 380:127–143
50. **Oomura Y, Nishino H, Karadi Z, Aou S, Scott TR** 1991 Taste and olfactory modulation of feeding related neurons in behaving monkey. Physiol Behav 49:943–950
51. **Dunn-Meynell AA, Routh VH, Kang L, Gaspers L, Levin BE** 2002 Glucokinase is the likely mediator of glucosensing in both glucose-excited and glucose-inhibited central neurons. Diabetes 51:2056–2065
52. **Elias CF, Aschkenasi C, Lee C, Kelly J, Ahima RS, Bjorbæk C, Flier JS, Saper CB, Elmquist JK** 1999 Leptin differentially regulates NPY and POMC neurons projecting to the lateral hypothalamic area. Neuron 23:775–786
53. **Elmquist JK** 2001 Hypothalamic pathways underlying the endocrine, autonomic, and behavioral effects of leptin. Physiol Behav 74:703–708
54. **Spiegelman BM, Flier JS** 2001 Obesity and the regulation of energy balance. Cell 104:531–543
55. **Ferin M, Van Vugt D, Wardlaw S** 1984 The hypothalamic control of the menstrual cycle and the role of endogenous opioid peptides. Recent Prog Horm Res 40:441–485
56. **Bicknell RJ** 1985 Endogenous opioid peptides and hypothalamic neuroendocrine neurones. J Endocrinol 107:437–446
57. **Spanagel R, Weiss F** 1999 The dopamine hypothesis of reward: past and current status. Trends Neurosci 22:521–527
58. **Kelly MJ, Lagrange AH** 1998 Nontranscriptional effects of estradiol in neuropeptide neurons. Curr Opin Endocrinol Diabetes 5:66–72
59. **Minami T, Oomura Y, Nabekura J, Fukuda A** 1990 17β-Estradiol depolarization of hypothalamic neurons is mediated by cyclic AMP. Brain Res 519:301–307
60. **Geary N** 2001 Estradiol, CCK and satiation. Peptides 22:1251–1263